2006

3-PG Productivity Modeling of Regenerating Amazon Forests: Climate Sensitivity and Comparison with MODIS-Derived NPP

Joseph D. White

Neal A. Scott

Adam I. Hirsch

Steven W. Running
University of Montana - Missoula, steven.running@umontana.edu

3-PG Productivity Modeling of Regenerating Amazon Forests: Climate Sensitivity and Comparison with MODIS-Derived NPP

Joseph D. White*

Department of Biology, Baylor University, Waco, Texas

Neal A. Scott and Adam I. Hirsch+

Woods Hole Research Center, Woods Hole, Massachusetts

Steven W. Running

School of Forestry/Numerical Terradynamic Simulation Group, University of Montana, Missoula, Montana

Received 15 September 2004; accepted 13 July 2005

ABSTRACT: Potential forest growth predicted by the Physiological Principles in Predicting Growth (3-PG) model was compared for forest and deforested areas in the Legal Amazon to assess potential differing regeneration associated with climate. Historical deforestation and regeneration have occurred in environmentally marginal areas that influence regional carbon sequestration estimates. Effects of El Niño–induced drought further reduce simulated production by decreasing soil water availability in areas with shallow

* Corresponding author address: Joseph D. White, One Bear Place #97388, Dept. of Biology, Baylor University, Waco, TX 76798.
E-mail address: Joseph_D_White@baylor.edu
+ Current affiliation: Cooperative Institute for Research in Environmental Sciences, University of Colorado, Boulder, Colorado.

soils and high transpiration potential. The model was calibrated through comparison of literature biomass and with satellite-based estimates. Net primary productivity (NPP) for mature Amazonian forests from the 3-PG model was positively correlated ($r^2 = 0.77$) with a Moderate Resolution Imaging Spectroradiometer (MODIS)-derived algorithm, though with some bias. Annual total NPP for the study area using a 1961–90 average climatology was 4.6 Pg C yr^{-1}, which decreased to 4.2 Pg C yr^{-1} when simulated with climate from the severe 1997/98 El Niño event. From a regional analysis, results showed that biomass accumulation is almost entirely controlled by the availability of soil water. Also, areas currently forested in the eastern Amazon are more sensitive to extreme El Niño–induced drought than southern areas with the greatest deforestation extent.

KEYWORDS: Net primary production; MODIS; Climate variability; El Niño; Amazon; Water limitation

1. Introduction

Forests in the Brazilian Amazon basin are cleared for a variety of purposes, ranging from small-scale agriculture to vast cattle grazing. Studies using satellite imagery report that on the order of 10 000 to 30 000 km^2 are cleared in the Brazilian Amazon basin each year, releasing 0.1–0.3 Pg C (1 Pg $= 1 \times 10^{15}$ g) per year (Skole and Tucker 1993; Houghton et al. 2000). However, cleared land utilized for agriculture generally depletes nutrient stores, particularly phosphorus, slowing regeneration by woody species from 5 to 20 yr following abandonment (Fearnside and Guimarães 1996; Müller et al. 2004). Woody plant regeneration on abandoned land is important for regional carbon budgets as uptake of carbon dioxide from the atmosphere by these forests regrowing is estimated to account for 0.06 Pg C yr^{-1} over the last two decades (Houghton et al. 2000; Hirsch et al. 2004).

Though less dramatic than the sudden release of carbon from deforestation, regrowing forest can accumulate aboveground biomass at a rate of 5.0 to 10.0 Mg of dry matter per hectare (1 ha $= 10\,000$ m^2) per year (Uhl et al. 1988; Brown and Lugo 1990), equivalent to roughly 2.5 to 5.0 Mg of carbon. Earlier studies suggest that the current annual carbon uptake by regrowing forests is small relative to deforestation loss to the atmosphere but that this rate will increase as more land is abandoned in the future (Salimon and Brown 2000; Fearnside and Guimarães 1996).

Previous simulation studies indicate that climatic factors such as radiation, precipitation, temperature, and available soil moisture are important predictors of primary production in tropical forests (Raich et al. 1991; Potter et al. 1998; Tian et al. 1998; Asner et al. 2000; Running et al. 2004). During El Niño events, precipitation is reduced along a west–east gradient with associated decreases in runoff and soil water storage (Zeng 1999). Forests are impacted most by soil moisture depletion (Potter et al. 2001); however, deep rooting by Amazonian forests mitigate drought stress by providing access to stored soil water in some areas (Nepstad et al. 1994; Potter et al. 1998). Few simulation studies have investigated regional patterns in above- and belowground allocation associated with large-scale climate patterns. Since deforestation in the Amazon basin has been concentrated in the seasonally dry south and east, we explore whether forest

regrowth in the "arc of deforestation" may be more vulnerable than other parts of the basin to climatic constraints, particularly moisture stress.

The forest model Physiological Principles in Predicting Growth (3-PG; Landsberg and Waring 1997) is utilized here to examine environmental controls on productivity. This model estimates production, biomass accumulation, and allocation from climate and soil factors as a "bottom-up" approach. Simulated production values are compared to Moderate Resolution Imaging Spectroradiometer (MODIS) net primary productivity (NPP)-derived values from Running et al. (Running et al. 2004), which are inferred from satellite data as a function of observed solar radiation absorption as a "top-down" approach. El Niño–induced climatic shifts decrease production in the Amazon basin through pervasive drought (Fearnside 1995; Tian et al. 1998; Asner et al. 2000) and are simulated here for the severe 1997/98 El Niño event. Deforestation maps are utilized to separate areas into deforested and forested categories for analysis to assess spatial variability in production, physiological controls of growth, and climate impacts associated with location and disturbance.

2. Methods

2.1. Description of the 3-PG model

The 3-PG model is based on simplified relationships of plant interaction with climate and soil and has been shown to accurately predict production biomass at a variety of scales (cf. Coops et al. 1998; White et al. 2000). In this model, production is primarily driven by the absorption and "utilization" of incident radiation. Photosynthetically active radiation ($\phi_{p.}$) is estimated from shortwave radiation assuming that 50% of this radiation was in the photosynthetically active radiation (PAR) range (McCree 1972) and absorbed photosynthetically active radiation (APAR; $\phi_{\text{p.a.}}$) is derived from Beer's law. The leaf area index (LAI) used to calculate $\phi_{\text{p.a.}}$ is derived from the amount of foliage biomass present at the end of each month (a balance between new foliar growth and fixed leaf litterfall). Updated leaf biomass values are multiplied by specific leaf area (SLA) to derive a new monthly LAI value.

The utilized portion of absorbed APAR ($\phi_{\text{p.a.u.}}$) is obtained by reducing $\phi_{\text{p.a.}}$ by a series of physiological modifiers derived from environmental constraints that represent partial to complete stomatal closure with modifiers ranging between 0 and 1 (see Landsberg 1986; McMurtrie et al.1994; Runyon et al. 1994). The environmental factors include average air temperature [f(T)], mean daytime atmospheric vapor pressure deficit [f(VPD)], soil water availability [f(SW)], stand age, and site fertility. Volumetric soil water content balance (r_θ) is calculated as the difference between total monthly rainfall and evapotranspiration losses plus storage. The f(SW) is calculated from

$$f(\text{SW}) = \frac{1}{1 + [(1 - r_\theta)/m]^n},$$

where m and n are coefficients representing the soil water potential change to different textural classes (Landsberg and Waring 1997). Incoming precipitation is

either intercepted by foliage or is added to the soil water. Intercepted precipitation is assumed to be evaporated, and therefore lost from the system. Soil is treated as a single unit with plant accessibility to all water for the assumed soil depth. Soil water budgets are calculated as the net amount of nonintercepted precipitation minus transpiration estimated by the Penman–Monteith equation.

Each month, the fraction of $\phi_{\text{p.a.}}$ actually utilized ($\phi_{\text{p.a.u.}}$) is determined by the most limiting environmental variable. Gross primary production (GPP) is calculated by multiplying $\phi_{\text{p.a.u.}}$ by a canopy quantum efficiency coefficient (α_c) derived from literature or observed values. The major generalization of 3-PG is that NPP in forests is a fixed fraction of GPP and is set at 0.45 (Landsberg and Waring 1997; Waring et al. 1998).

The model partitions NPP into root and aboveground foliage and stem mass. The fraction of total NPP allocated to root growth increases from 0.2 to 0.8 as the ratio $\phi_{\text{p.a.u.}}/\phi_{\text{p.a.}}$ decreases from 1.0 to 0.2. Remaining biomass is assigned to stems based on the following allometric relationship:

$$W_s = \frac{fs_{2\text{cm}}}{c}\,\text{DBH}_{\text{avg}}^{c},$$

where W_s is stem mass, $fs_{2\text{cm}}$ is the partitioning ratio of foliage and stems at a diameter at breast height (DBH) of 2 cm, and DBH_{avg} is the stand average DBH calculated monthly. The coefficient c is derived from

$$c = \frac{\log_e\left(fs_{20\text{cm}}/fs_{2\text{cm}}\right)}{\log_e(10)},$$

where $fs_{20\text{cm}}$ is the foliage to stem partition when the DBH of a tree is 20 cm. Aboveground biomass accumulation (ABA) is the net amount of W_s over a given simulation time. Foliage mass is calculated as the remainder of NPP after allocation to roots and stems.

2.2. Initial model parameters

As the 3-PG model was originally developed for plantation forests, initial values for 3-PG parameters were extracted from the primary literature to characterize a generic tropical species (Table 1). Parameters modified from the original model for these simulations are grouped into three classes: allometry, physiology, and biomass turnover. Initial stand tree density, stem/DBH relationships, SLA, and proportion of bark and branch biomass of stems were based on field studies recently conducted in Amazonia (Nepstad et al. 2002; Laurence et al. 1999; Chambers et al. 2000). Initial parameter values include maximum leaf turnover that was set at 0.9 yr^{-1}, and partitioning between leaves and stem set to 1:1, in order to reproduce the general range of LAI values observed across the Amazon (Honzak et al. 1996; Saldarriaga and Luxmoore 1991). The root turnover rate was set to 0.02 yr^{-1} and includes fine and coarse roots, with coarse roots contributing the most biomass and therefore controlling turnover rate (Nepstad et al. 1994).

A broad temperature growth range was selected with a minimum of 5°C, a maximum of 40°C, and an optimum of 27°C based on the climatic conditions commonly occurring in tropical forests (Eamus 1999). Stomatal closure due to

Table 1. Parameter values for the 3-PG simulation. Literature sources are shown.

Parameter	Value	Reference
Foliage:stem partitioning when diameter = 2 cm (fs_{2cm}) (dimensionless)	1.00	Laurence et al. (1999)
Foliage:stem partitioning when diameter = 20 cm (fs_{20cm}) (dimensionless)	0.15	Laurence et al. (1999)
Maximum fraction of NPP to roots (dimensionless)	0.8	Nepstad et al. (1994)
Minimum fraction of NPP to roots (dimensionless)	0.2	Nepstad et al. (1994)
Minimum temperature for growth (°C)	10.0	Eamus (1999)
Optimum temperature for growth (°C)	27.0	Eamus (1999)
Maximum temperature for growth (°C)	40.0	Eamus (1999)
Quantum conversion efficiency (α_c) (mol C mol $\phi_{p.a.u.}^{-1}$)	0.0033	Carswell et al. (2000)
Maximum monthly litterfall rate ($month^{-1}$)	0.03	Neptstad et al. (2002)
NPP:GPP (dimensionless)	0.45	Landsberg and Waring (1997)
Stomatal response to VPD (k) (kPa^{-1})	0.0125	Granier et al. (1996)
Maximum stem mass per tree at 1000 trees per ha (kg per tree)	300.0	Nepstad et al. (2002)
SLA (m^2 kg C^{-1})	20.0	Carswell et al. (2000)
Beer's law extinction coefficient (LAI^{-1})	0.7	Saldarriaga and Luxmoore (1991)
Canopy precipitation interception (cm LAI^{-1})	0.15	Nepstad et al. (2002)

vapor pressure deficit [f(VPD)] is modeled in 3-PG as a negative exponential function [i.e., $f(\text{VPD}) = e^{-k*\text{VPD}}$]. The exponential coefficient (k) determines the model's sensitivity to VPD. In these simulations k was assigned a value 0.0125 per kilopascal, or one-quarter of the default value of 0.05 (Landsberg and Waring 1997), similar to values measured for tropical trees (Granier et al. 1996). This lower VPD coefficient shifted dominance of physiological control of growth to soil moisture. Physiological parameter values for tropical tree species, including canopy quantum efficiency ($\alpha_c = 0.033$ mol C mol photons^{-1}) and specific leaf area were obtained from Carswell et al. (2000). In the analysis, Pearson's correlation coefficients were calculated for simulated NPP, ABA, all physiological modifiers, and solar radiation to assess influence of these environmental factors on forest growth.

2.3. Climate data

Our study area is the Legal Amazon defined here by Potter and Brooks-Genovese (Potter and Brooks-Genovese 2003) for which all final carbon budget values are calculated. The Legal Amazon includes the Brazilian states of Acre, Amapá, Amazonas, Pará, Rondônia, Roraima, Mato Grosso, Maranhão, and Tocantins (IBGE 1991). Temperature and precipitation data were derived from the 1961–90 East Anglia Climatic Research Unit (CRU) 0.5° × 0.5° global monthly averaged climatology (New et al. 1999), available through the Intergovernmental Panel on Climate Change (IPCC) at their Web site (http://ipcc-ddc.cru.uea.ac.uk). These data were averaged for the entire record period to derive 12 monthly climate input grids of maximum and minimum temperature and precipitation for the 3-PG simulation. Radiation data were derived from monthly averages of Dr. Rachel Pinker's 1990–92 surface shortwave radiation dataset (Pinker and Laszlo 1992). These radiation data, produced as part of the National Oceanic and Atmospheric Admin-

istration/National Aeronautics and Space Administration (NOAA/NASA) Pathfinder project, also have a scale of 0.5° × 0.5° and are provided as part of the NASA Large-Scale Biosphere-Atmosphere (LBA) project.

VPD was calculated from the minimum and maximum temperatures based on the equations of Murray (1967). To determine the reliability of this method, data from the Anglo-Brazilian Amazonian Climate Observation Study (ABRACOS) micrometeorology dataset from 1993 for the Reserva Jaru, near the Ji-Parana, Rondônia, forest site (approximately 11°S, 62°W; Gash and Nobre 1997) were compared with the CRU-derived values. ABRACOS data from April through October had VPD values ranging from 0.73 to 1.56 kPa compared to CRU-calculated values that ranged from 1.08 to 1.42 kPa. Seasonal trends were also similar, with both observed and modeled values from the increasing equivalently from the wet to dry season (Figure 1).

2.4. Soil texture

The 3-PG model requires soil texture information to calculate *f*(SW). We used previously derived soil texture categories (Potter et al. 1998) to initialize the soil texture categories (clay, clay-loam, sandy loam, and sand) needed for the 3-PG model, which required some interpretation as original texture categories were

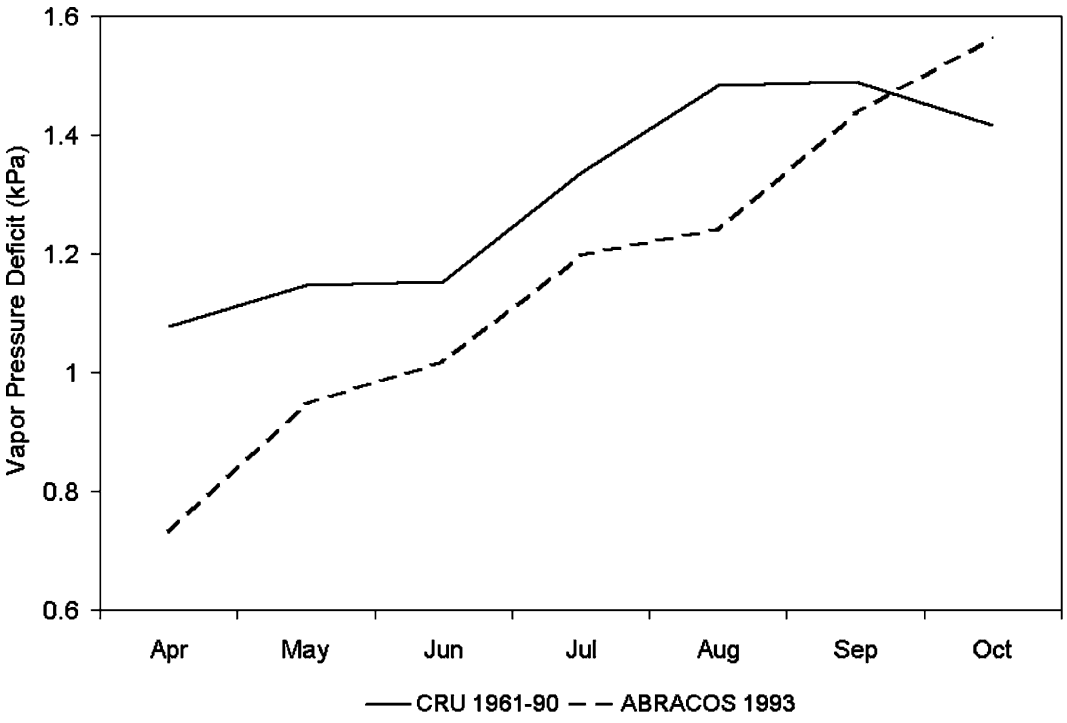

Figure 1. Comparison of observed and modeled vapor pressure deficit (kPa) values. Observed values are from the 1993 ABRACOS dataset (Gash and Nobre 1997) for the Reserva Jaru, near Ji-Parana, Rondônia. Modeled data are from the CRU monthly average values from 1961 to 1990.

based on clay content alone (FAO/UNESCO 1971). During the runtime of the 3-PG model, the m and n parameters important in the f(SW) calculation were changed dynamically for each grid cell based on the mapped soil texture with parameter values derived from Landsberg and Waring (1997).

2.5. Model comparison with MODIS NPP data

Annual global NPP values from 2000 to 2003 at a 1-km scale have been developed (Running et al. 2004; Zhao et al. 2005) from algorithms developed for the MODIS sensor. GPP is estimated from MODIS based on conversion of absorbed photosynthetically active radiation into carbon uptake modified by surface meteorological conditions suitable for photosynthesis. Gridded meteorological data such as temperature, vapor pressure deficit, and radiation are provided by the NASA Data Assimilation Office (DAO; http://polar.gsfc.nasa.gov/index.php; Atlas and Lucchesi 2000). From MODIS spectral data, GPP is estimated every 8 days. NPP is derived from GPP by subtracting autotrophic respiration of leaves, roots, and stems for different cover types as a function of biomass and temperature. Annual NPP is calculated as the summed value of NPP for a given year. Final annual NPP data are publicly available from the Numerical Terradynamics Simulation Group at the University of Montana's Web site (http://www.ntsg.umt.edu/) from which data were obtained for this study.

Model accuracy was assessed by linear regression analysis of the 3-PG simulation at 100 yr and MODIS NPP for 40 random, undisturbed forest points. The 100-yr age limit was selected because modeled carbon accumulation in forests increases slowly beyond this age (White et al. 2000) and represents the average mature forest accumulation rate in tropical forests (Guariguata and Ostertag 2001). Comparison of the NPP estimates involved extracting the maximum value within a 63 × 63 pixel window from the 2000–03 MODIS data. The window size was selected to scale the 1-km spatial resolution of the MODIS data to the 0.5° resolution of the data utilized for the 3-PG simulations. Previous research has shown that 3-PG models maximum site production (Coops et al. 1998); therefore, selection of the maximum MODIS NPP values over the 4-yr period was assumed to represent equivalent maximum production.

2.6. El Niño scenario

In 1997/98, the Amazon basin experienced perhaps the strongest El Niño–Southern Oscillation event of the twentieth century (Williamson et al. 2000; McPhaden 1999), causing decreased rainfall during the wet season and extending the dry season in much of the Amazon basin. To assess the impact of El Niño–induced drought on potentially regenerating forests in the Amazon, NPP was simulated with 3-PG for 20 yr utilizing 1) CRU monthly averaged climate from 1961 to 1990 and 2) monthly averaged climate from 1997 to 1998 (New et al. 1999). The simulations were not intended to assess true El Niño events but rather the influence of El Niño–related drought on forests. The two scenarios were assessed by calculating the following:

$$\mathrm{NPP}_{\Delta\mathrm{en}} = (\mathrm{NPP}_{\mathrm{elniño}} - \mathrm{NPP}_{61-90})/\mathrm{NPP}_{61-90},$$

where $NPP_{elniño}$ is NPP at year 20 in each grid cell, using the 1997/98 data, and $NPP_{61–90}$ is NPP using the average climatology for 1961–90.

To study the impact of rooting depth on production using 3-PG, we reran all model scenarios increasing soil depth to 5 m from the base run value of 2 m. The 3-PG model does not consider the impact of seasonal flooding on productivity (i.e., we are simulating "terra firme" forests). Values of $NPP_{\Delta en}$ were recalculated from these simulations to assess combined effects of climate and plant water availability.

2.7. Comparison of deforested and forested areas

Deforested and undisturbed forested areas within the Legal Amazon were mapped from 1992 data with 8-km resolution data obtained from the Tropical Rain Forest Information Center (TRFIC) located at Michigan State University (http://www.globalchange.msu.edu/trfic/). A geographical mask of these data was applied to limit analysis to the Legal Amazon (Potter and Brooks-Genovese 2003). These data were projected to a geographic projection with a 0.5° ground resolution where any pixel mapped as deforested at the 8-km scale was also designated as a deforested pixel at the 0.5° resolution. The purpose of this process was to identify pixels affected by disturbance rather than to quantify area.

Utilizing the TRFIC deforestation GIS data layer for 1992, 80 random sample points were extracted from the 3-PG-simulated NPP and root allocation outputs for 20 yr with 40 points in the deforested and forested areas, respectively. Also, 80 random data points were extracted from the $NPP_{\Delta en}$ for deforested and forested areas to compare impacts of El Niño and soil depth on forest productivity. All statistical analyses such as linear regression and analysis of variance (ANOVA) assume that α is equal to 0.05 utilizing SPSS software (SPSS, Inc., Chicago, Illinois).

3. Results

3.1. Environmental controls of forest production

Pearson's coefficient for correlation values between ABA after 20 yr with climate variables and model physiological modifiers are shown in Table 2. The factor most responsible for aboveground biomass accumulation variability across the study area is soil moisture availability (Table 2; Figure 2). However, 3-PG predicts no difference in ABA with soil texture despite the difference in hydraulic properties of different texture classes in 3-PG. Only in locations where soil water is not limiting, generally with annual rainfall greater than 2000 mm, do other factors begin to control biomass variability. Under conditions with no moisture limitation, radiation is highly correlated with predicted aboveground biomass (Figure 3).

3.2. Spatial variability of forest production

The output of simulations of NPP at 20 and 100 yr were mapped representing the potential production of regenerating and mature forests, respectively. NPP after 20 simulation years and 2-m rooting depth is shown in Figure 4 (units are Mg dry matter ha^{-1} yr^{-1}). The total NPP for the study region is 9.2 Pg of dry matter, or 4.6 Pg C yr^{-1}, assuming a forest carbon content of 50%. The NPP pattern after 100 yr

Table 2. Pearson's correlation coefficient values for simulated aboveground biomass accumulation after 20 yr and environmental factors plus derived modifiers from the 3-PG model.

Variable	Pearson's correlation coefficient
Precipitation (mm yr^{-1})	0.89
Minimum temperature (°C)	0.57
Maximum temperature (°C)	0.19
Shortwave radiation (MJ m^{-2} yr^{-1})	–0.45
Soil water holding capacity to 2 m (mm)	0.14
f(SW)	0.98
f(VPD)	0.35
f(*T*)	0.46

of growth is nearly identical, though slightly lower than the value for 20 yr of growth as the 3-PG model accounts for reduction in stomatal conductance associated with older trees.

The predicted ABA in the Brazilian Amazon basin after 20 yr of simulation (representing forest regeneration) clearly decreases from north to south (Figure 5). The maximum predicted aboveground biomass is 174 Mg of dry matter per hectare (Mg DM ha^{-1} = 1×10^6 gDM ~5×10^5 g C) with a mean value of 102 Mg DM ha^{-1}. Predicted total biomass at 20 yr has a spatial pattern similar to NPP, with maximum biomass of 272 Mg DM ha^{-1}, and mean of Mg DM ha^{-1}.

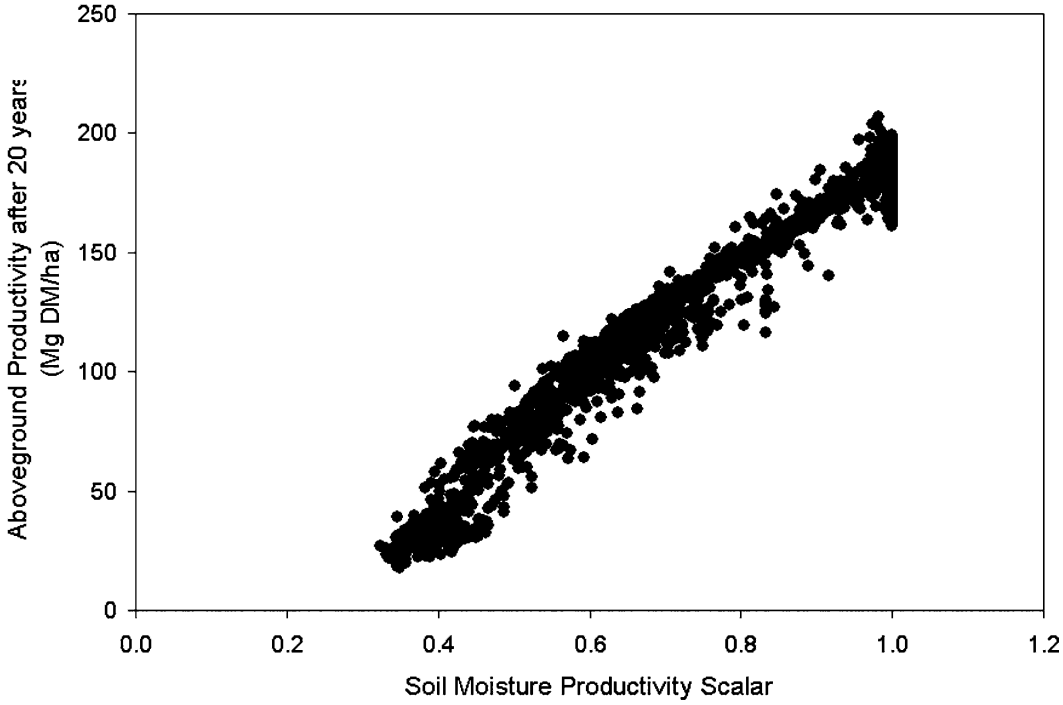

Figure 2. The 20-yr ABA vs the 3-PG soil moisture availability scalar.

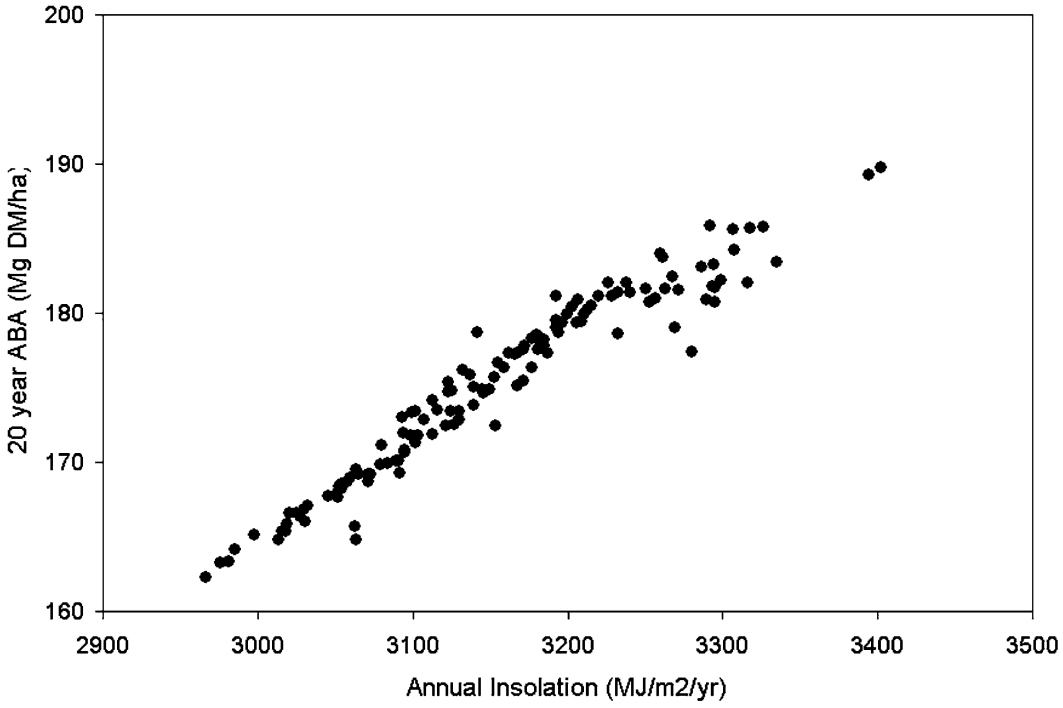

Figure 3. The 20-yr ABA vs shortwave radiation flux for pixels with no simulated soil moisture stress.

For comparison to 20 yr ABA, we include a map (Figure 6) of aboveground forest biomass after 100 yr of regrowth, when forest biomass may be approaching mature forest values (Guariguata and Ostertag 2001). The pattern is very similar to the 20-yr simulation, with high values in the northwest, and lower values in the central and southeastern portions of the basin. The maximum predicted ABA is 690 Mg DM ha^{-1} (equivalent 345 Mg C ha^{-1}, assuming that forests are 50% carbon), with a mean of 435 Mg DM ha^{-1} and standard deviation of 165 Mg DM ha^{-1}.

Soil depth influences NPP differently for deforested and forested areas (Table 3). In model simulations with 2-m soil depths, NPP values are significantly exaggerated between deforested and forested areas, but not with 5-m soil depth simulations. However, only forested areas have different simulated NPP when compared between 2- and 5-m soil depths. Root allocation under all conditions was not different.

Figure 7 shows the ratio of ABA after 20 yr for 5–2-m soil depth simulations. The root/shoot ratio across the basin reflects the dynamic allocation between aboveground and belowground components as a function of productivity. As a result, the root fraction of total biomass is much higher in stands with productivity constraints and lower biomass (Figure 8). Assumed soil depth and plant water availability also influence root partitioning. This shows that root partitioning varies spatially with more biomass allocated to roots in the southern region under an assumed 2-m soil depth. In central regions, root partitioning was greater with

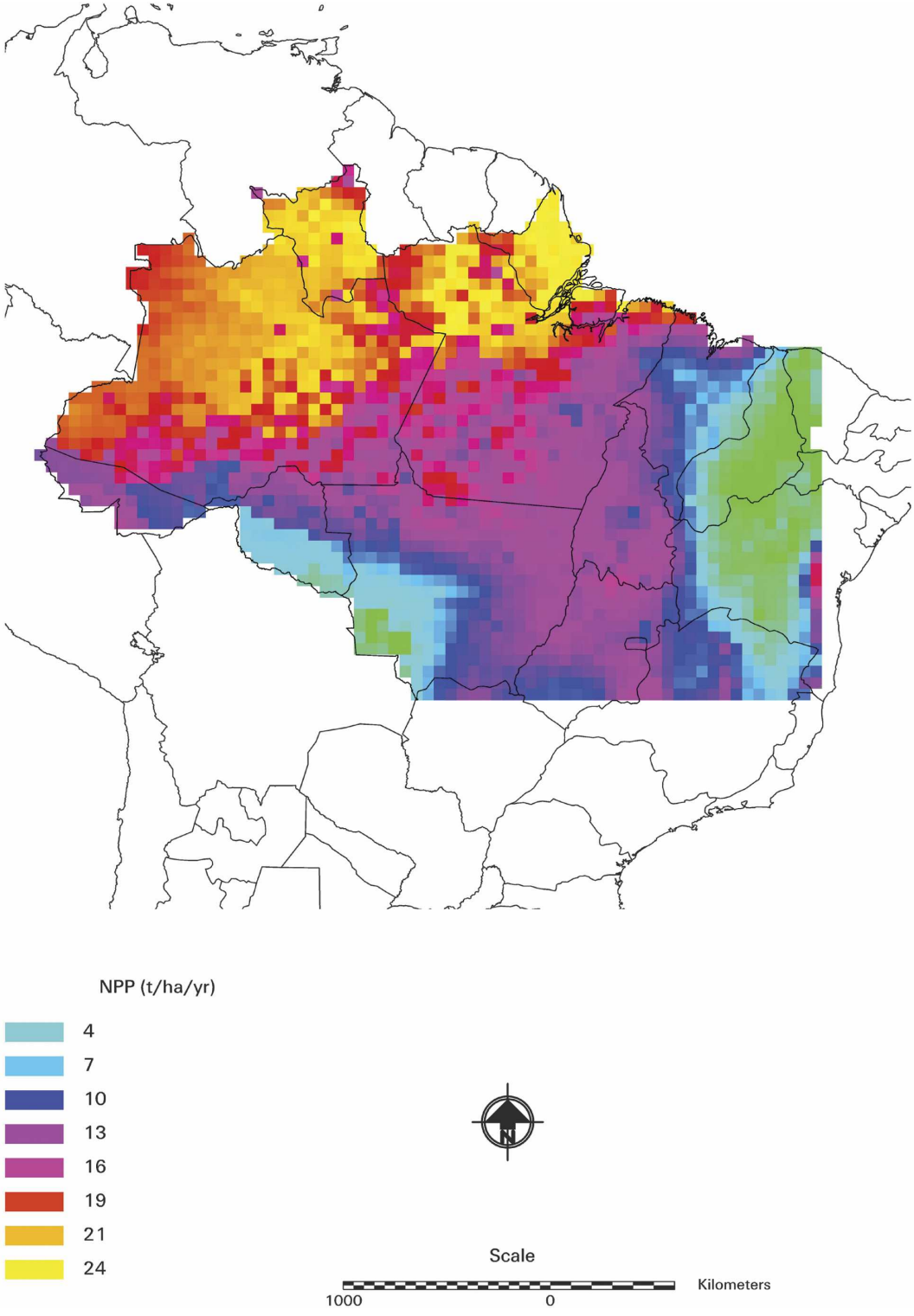

Figure 4. 3-PG-simulated NPP in year 20, assuming a 2-m rooting depth.

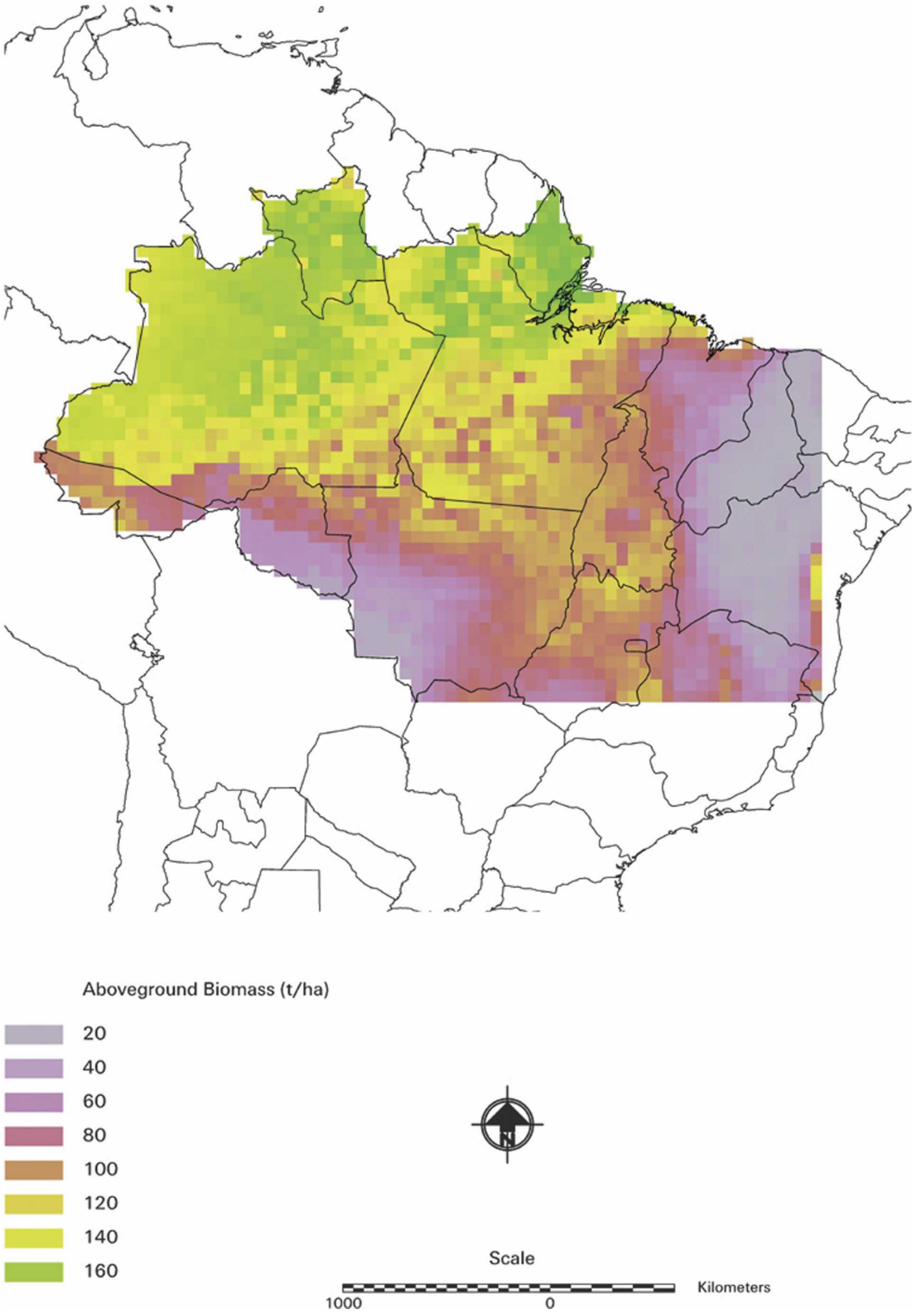

Figure 5. 3-PG-predicted ABA (Mg dry matter per ha) after 20 yr of simulation.

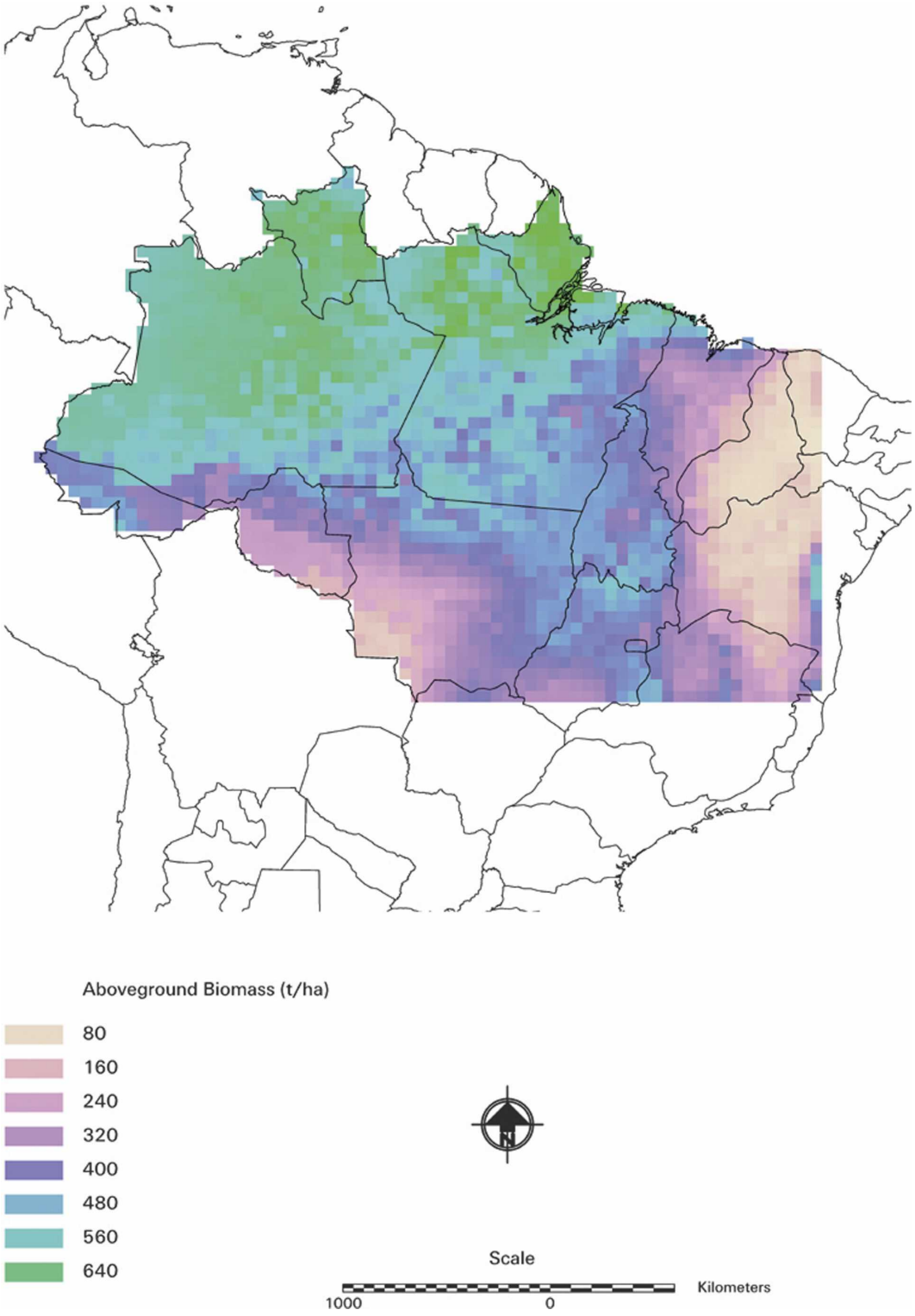

Figure 6. Same as in Figure 5, but after 100 yr.

Table 3. Results of ANOVA tests for comparisons of NPP at 20 yr for deforested and forested areas under different model conditions. Significant results are indicated by an asterisk ($p < 0.05$) while NS represents nonsignificant results. Where significant results were found, impacts are described.

Test	Results	Impact
NPP		
2 m	*	NPP higher in forested areas
5 m	NS	
Deforested: 2 vs 5 m	NS	
Forested: 2 vs 5 m	*	Forested areas with deeper soils had higher NPP
Root partitioning		
2 m	NS	
5 m	NS	
Deforested: 2 vs 5 m	NS	
Forested: 2 vs 5 m	NS	
$NPP_{\Delta en}$		
2 m	NS	
5 m	*	Deforested areas had less NPP during El Niño years
Deforested: 2 vs 5 m	NS	
Forested: 2 vs 5 m	*	Forested areas with deeper soils had less NPP during El Niño years

2-m soil depth. However, point comparisons reveal no significant difference in root allocation for any simulation comparisons (Table 3).

3.3. Comparison with MODIS NPP data

Simulated NPP at 100 yr compared favorably to maximum MODIS NPP data from 2000 to 2003 (Running et al. 2004) with high positive correlation ($r^2 = 0.77$; Figure 9). Values were related 1:1, indicating accurate scaling of NPP across the basin. However, the 3-PG model overestimates NPP by an average 1.0 Mg C ha^{-1} yr^{-1} ($p < 0.05$) when compared with the MODIS-derived NPP. Further analysis of the MODIS productivity data for 2000–03 also indicates a basin average NPP:GPP of 0.47, slightly higher than the 0.45 value utilized in the 3-PG simulations.

3.4. The impact of El Niño–induced drought

The drought simulated utilizing the 1997/98 El Niño climate data with a 2-m rooting depth had the largest impact on predicted total basin NPP, reducing the value to 4.2 Pg C yr^{-1}. The simulated impact of El Niño–induced drought was less severe for a 5-m-deep soil, reducing NPP to 4.4 Pg C yr^{-1} relative to the average climate simulations. The results of the ANOVA for $NPP_{\Delta en}$ values showed that rooting depth does not affect simulated NPP between El Niño drought and average climate years. Significant differences were found in $NPP_{\Delta en}$ between deforested and forested areas for 5-m soil depth simulations in which NPP is reduced under the El Niño drought scenario ($p < 0.05$; Table 3). This is due to the central forested region having only small differences in NPP relative to deforested regions to the southeast. Figures 10a and 10b illustrate the spatial variability of $NPP_{\Delta en}$, shown as a percentage, for 2- and 5-m soil depth simulations. Drought influences productivity as a gradient with eastern forests affected most.

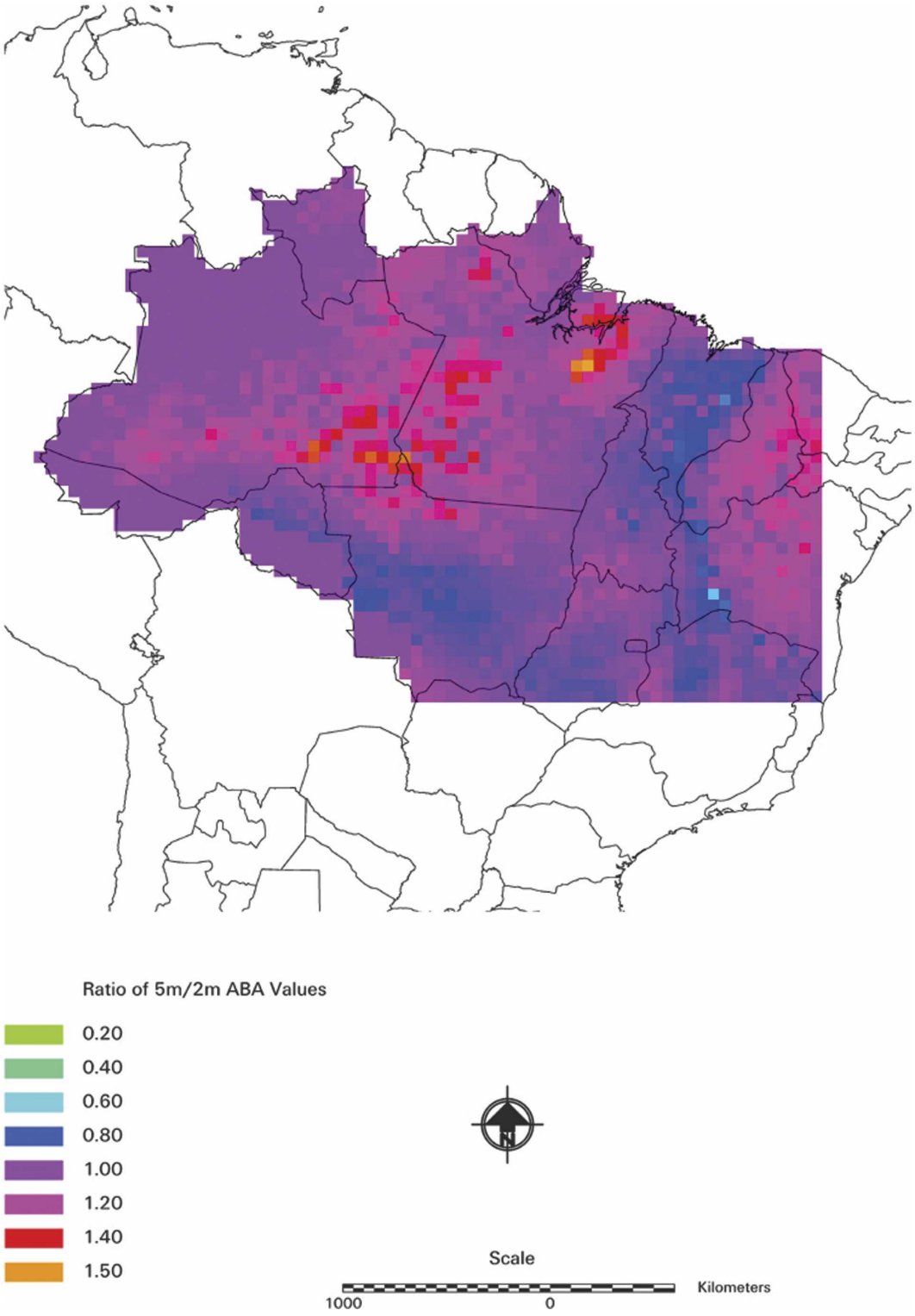

Figure 7. Ratio of 20-yr ABA using 5- vs 2-m rooting depths.

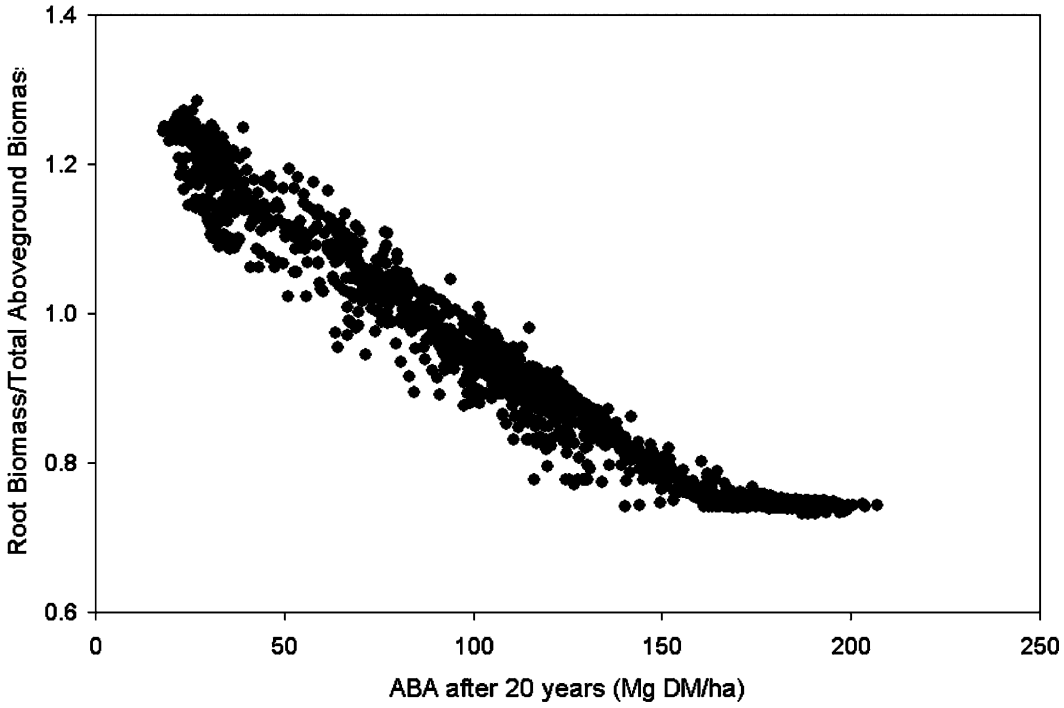

Figure 8. Root/total aboveground biomass ratio as a function of 20-yr simulated ABA.

4. Discussion

4.1. Environmental drivers

Temperature, especially monthly maximum temperature, varies little across the Amazon in the CRU 1961–90 climatology and has values close to the optimal temperature for plant growth in 3-PG. VPD potentially influences productivity in the basin because simulated VPD can exceed 2 kPa in some areas. However, the Pearson's correlation analysis did not show a large reduction in production (Table 2). Recent measurements from the ABRACOS campaign suggest that the relationship between stomatal conductance and VPD may be linear throughout the entire range of VPD (Roberts et al. 1996) rather than as an exponential function represented currently in 3-PG. Broadly, absorbed solar radiation is limiting in the Amazonian environment because of self-shading within canopies as a function of high LAI development and cloudiness associated with extreme rainfall amounts (Churkina and Running 1998; Running et al. 2004). Average LAI modeled by 3-PG was 4.2, which translates to an incoming radiation absorption rate of 95% assuming an extinction value of 0.70. However, recent observations by Emmons and DuBois (Emmons and DuBois 2003) indicate a potentially higher extinction rate of 0.88, which if used here would translate to 98% of radiation absorbed at modeled LAI values.

The results of these simulations also indicate that when rainfall exceeds 2000

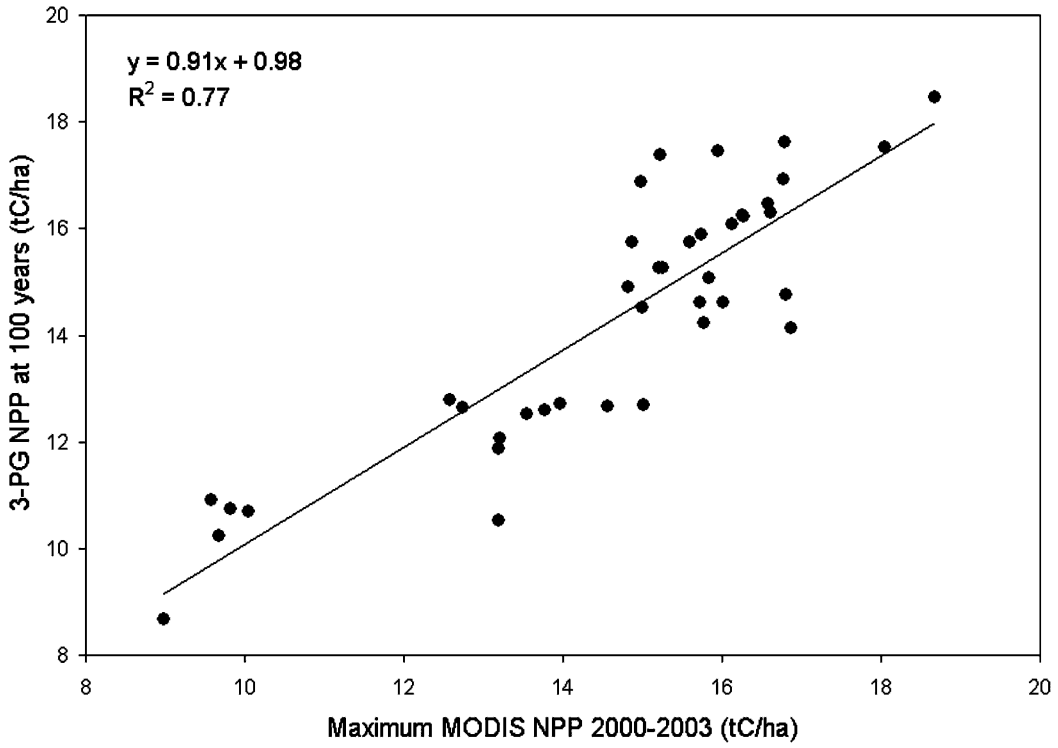

Figure 9. Linear regression of 3-PG-predicted NPP after 100 yr and maximum MODIS-derived NPP for 2000–03 from Running et al. (Running et al. 2004).

mm yr^{-1}, radiation limits ABA as a result of persistent cloudiness and reduced solar radiation flux.

Our application of 3-PG identifies the overwhelming role of soil water represented by the *f*(SW) in controling NPP and aboveground biomass accumulation in the basin, and is consistent with previous studies stating that variability in Amazon rainfall can have significant impacts on the global carbon budget through altered forest productivity. While it is counterintuitive that biomass accumulation should be limited by water availability in the rain forests of the Amazon, precipitation across the basin is very seasonal, so that soil moisture depletion occurs during the dry season (roughly June–October), especially south of the Amazon River. Figure 11 shows the fraction of total rainfall that falls during the months of June–October across the basin. Although June–October represents 42% of the year, dry season precipitation in much of the basin represents less than 20% of total annual rainfall. As the length of the dry season is inversely related to stem density broadly across the Amazon forest (Mahli et al. 2002), it therefore influences stand biomass, self-thinning, and coarse woody debris accumulation.

Combined patterns of precipitation and soil depth influence soil moisture controls on plant production. In 3-PG, soil moisture stress is affected by precipitation inputs and soil depth. For example, low precipitation and deep soils result in low *f*(SW) and production as less water fills a larger soil volume. The mapped ratio of

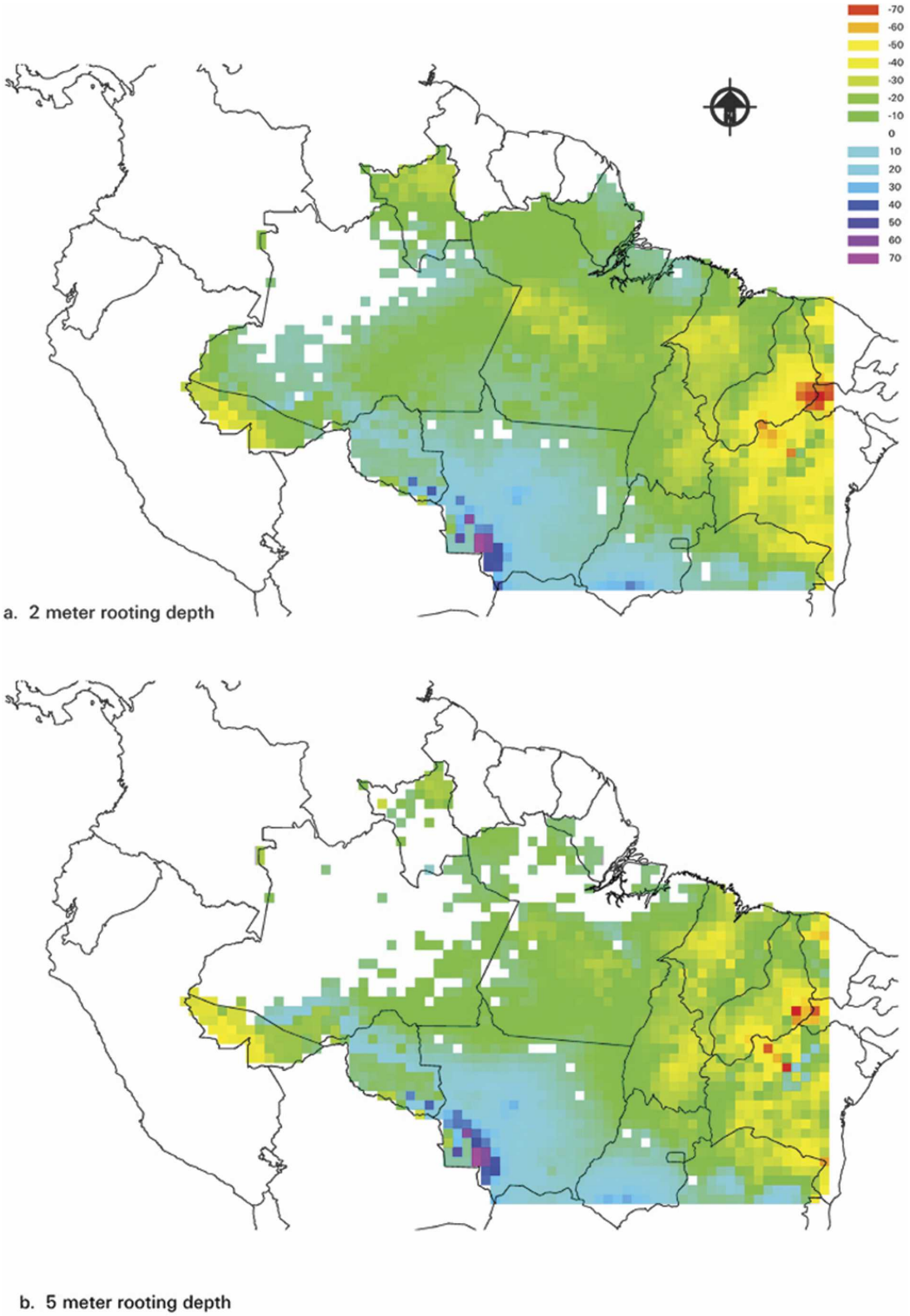

Figure 10. Percentage change in 3-PG-estimated NPP due to the 1997/98 El Niño–induced drought.

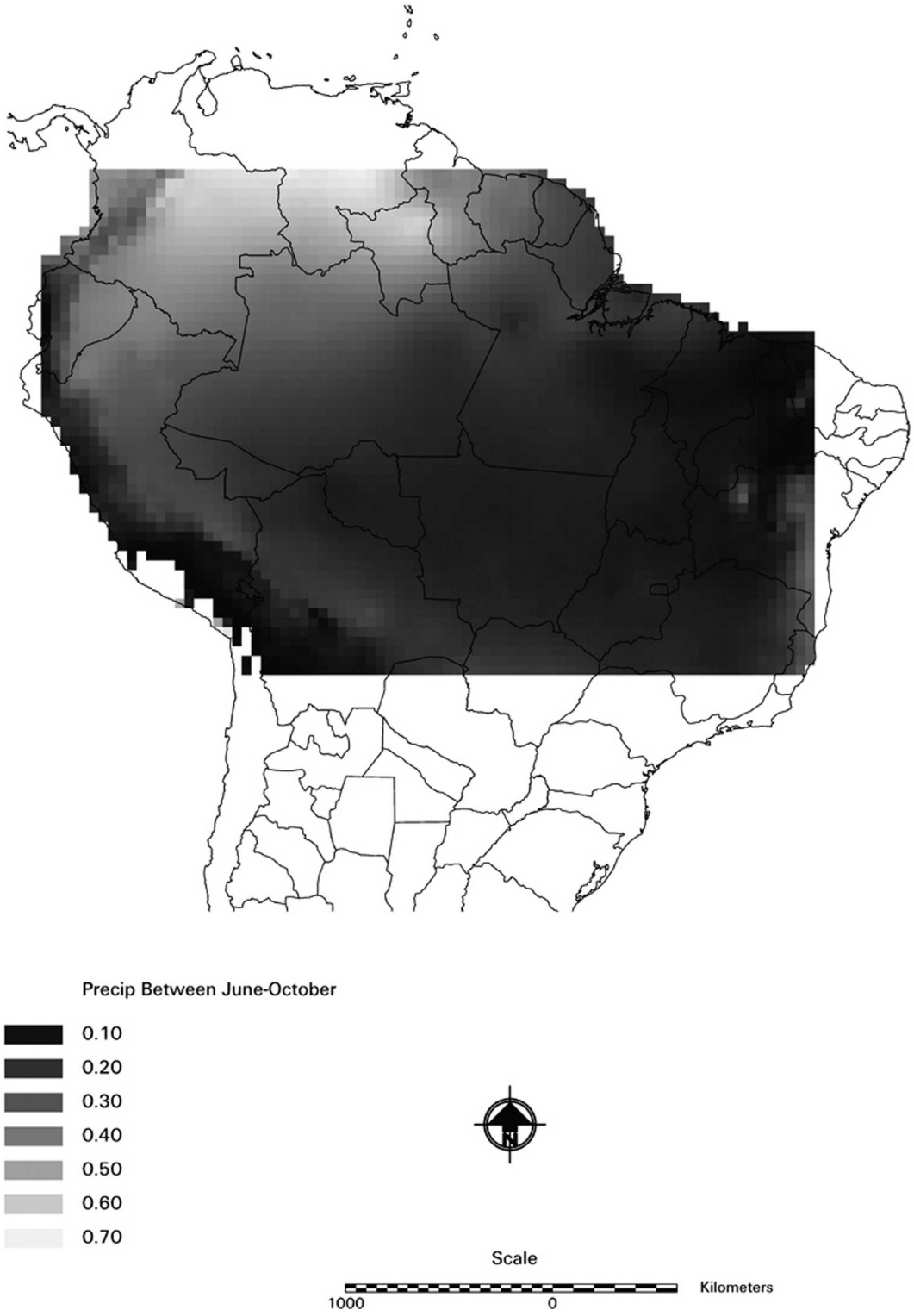

Figure 11. Fraction of precipitation falling between Jun and Oct.

ABA between 5- and 2-m simulations (Figure 7) illustrates this effect where southern regions of the Amazon, which are most impacted by deforestation, have lower production if soils are deep. This is in contrast to central Amazon, where deeper soils result in greater productivity and similar to results by Potter et al. (Potter et al. 2001). Soil depth in this region that increases soil water reservoirs accumulated during the wet season. However, recent observations of seasonal soil moisture in Pará by Goulden et al. (Goulden et al. 2004) show that most water uptake by trees appears to be derived from the soil horizon < 2 m. One conclusion that could be drawn from these results is that long-term measurements of soil moisture are important for a mechanistic interpretation of production response to climate variation both spatially and temporally (Jipp et al. 1998; Hodnett et al. 1996).

Rooting depth has been identified as an important factor in determining the length of the growing season in the Amazon (Nepstad et al. 1994). Forests that might be expected to shed their leaves based on soil water availability in the top meter or two continue to grow because of deep rooting. In some areas in the southern portion of the basin, ABA can be enhanced by 50% of this change. Because simulated biomass accumulation is sensitive to soil depth in areas with limited soil water availability, quantifying forest access to stored soil water as a function of climate and forest age would improve the reliability of forest carbon budget simulations. The 3-PG simulations also suggest that current deforestation, which occurs primarily along the arc of deforestation in the Amazonian states of Para, Mato Grosso, and Rondônia, is taking place in the forests most exposed to soil moisture stress during the dry season and is thus least resilient to disturbance (Table 3). This stress may only occur on shallow soils sites as deforested simulations with deep soils were not different from forested sites. This is because shallow soils hold less water and are depleted faster through evapotranspiration. An interesting finding for these simulations is the lack of root allocation difference within the basin. While other factors such as nutrient exploitation may induce greater root growth, soil water and other climate drivers do not inherently change modeled allocation patterns appreciably.

Soil nutrients were not included in these simulations because continuous data do not exist at an appropriate scale and accuracy for the basin. Soil nutrient properties may vary spatially on the scale of meters, while gridded soil data have a spatial resolution of kilometers at best. Laurence et al. (Laurence et al. 1999) suggest that soil fertility can explain a significant proportion of biomass variability on heavily weathered Amazon soils. However, the range of biomass values on low to high fertility sites are very similar (Mahli et al. 2002), indicating that inclusion of soil nutrient information for productivity modeling in the Amazon may improve site accuracy with a limited affect on regional average predictions.

4.2. Comparison of forest production estimates

Spatially explicit applications of models such as Carnegie–Ames–Stanford Approach (CASA) (Potter et al. 1998, 2001; Asner et al. 2000), Terrestrial Ecosystem Model (TEM) (Tian et al. 1998), or 3-PG (Hirsch et al. 2004) help identify mechanisms that cause observed interannual variability in the atmospheric carbon burden. The 3-PG-simulated values of NPP values are comparable to the results presented in Potter et al. (Potter et al. 1998), though the maximum 3-PG NPP is

slightly higher than the maximum NASA–CASA NPP (18 versus 14 Mg C ha^{-1} yr^{-1}). This is similar to the results presented by Tian et al. (Tian et al. 1998), who found a range of 3.8–5.1 Pg C yr^{-1} from 1980 to 1994 for NPP in their "climate-only" scenarios (3-PG does not include the impact of CO_2 "fertilization"). Total NPP is also similar to the results of Asner et al. (Asner et al. 2000), who calculated a range of about 4.2 to 4.8 Pg C yr^{-1} from 1982 to 1993.

Likewise, ABA estimates for young and mature stands are comparable with published results. Young stands, defined here as the 20-yr 3-PG simulations, had mean a value of 123 (±52) Mg DM ha^{-1}. Global secondary tropical forests ABA may range from 50 to 200 Mg DM ha^{-1} (Brown and Lugo 1990; Feldpausch et al. 2004). Mature stands, defined as 100-yr simulations, had mean ABA values 435 (±165) Mg DM ha^{-1}, which are higher than observed average values of 318 (±11) Mg DM ha^{-1} reported by Baker et al. (Baker et al. 2004) for 59 forest plots. However, the plots utilized in that particular study included many sites from the upper drainage that are beyond the boundaries of the Legal Amazon.

4.3. Comparison with MODIS data

Initial comparison of 3-PG NPP with Running et al. (Running et al. 2004) annual MODIS NPP data showed that analysis of individual years had poor correspondence. However, high correlation was found when compared with maximum values from 2000–03 MODIS NPP data. This confirms that 3-PG models maximum potential production rather than actual yield for a specific time frame (Coops et al. 1998). Also, considerable variation was observed in the MODIS NPP data around the comparison sites representing local-scale variation in soil and vegetation canopy condition characteristics. This variation demonstrates that the MODIS-derived NPP product responds to environmental drivers at an annual time step.

Large production differences exist along the southern boundary of the Amazon as a function of climate and deforestation patterns, which are observable from space. The MODIS NPP data represent actual conditions of the forest integrating changes in canopy condition related to seasonal climate cycles and disturbance. Average MODIS NPP values for each of the 2000–03 dataset years with pooled means and standard errors for forested areas and deforested are 17.6 (±0.2) and 9.7 (±0.4) Mg C ha^{-1}, respectively. The deforested value of 9.7 Mg C ha^{-1} is considerably lower than the 3-PG value of 14.6 Mg C ha^{-1} at 20 yr. The difference between the 3-PG values at 20 yr and MODIS NPP in deforested areas is due to delayed natural reforestation. The 3-PG model does not include the temporal aspects of deforestation and subsequent land-use changes such as cattle ranching. Reforestation on pastures is soil limited because of increased soil bulk density, reduced nitrogen mineralization, and leached phosphorus as a function of livestock activity (Müller et al. 2004). The issue of soil and nutrient availability remains as a major research need for refinement of modeling in this region, particularly limited by the availability of spatial data and nutrient uptake studies by tropical species.

Both 3-PG and the MODIS NPP algorithms are climate-driven models that differ in their representation of carbon assimilation and allocation. For 3-PG, the NPP:GPP is assumed constant whereas the MODIS NPP algorithm varies autotrophic respiration by temperature and biomass. The constant NPP:GPP rela-

tionship forwarded by Landsberg and Waring (1997) in the 3-PG model has generated debate over its applicability across ecosystems. However, the average value of 0.47 derived from the analysis of the MODIS NPP and GPP data is within the range proposed by Landsberg and Waring (Landsberg and Waring 1997) value as well as the average value presented by Amthor (Amthor 2000) of 0.48. Chambers et al. (Chambers et al. 2004) report the ratio of autotrophic respiration to gross production from flux tower measurements in the central Amazon of 0.26 based on assumptions about belowground production and flux measurements under stable nighttime air conditions. This converts to a NPP:GPP ratio of 0.74 that is significantly higher than the 0.45 value utilized in our simulations. A constant NPP:GPP is useful for regional modeling to avoid adding unknown errors where considerable spatial variability exists. However, though the average MODIS-derived NPP:GPP ratio values were similar, spatial variance was noted that is likely to have a climatic driver, possibly temperature. Therefore, future model comparisons of 3-PG and MODIS productivity simulations will focus on the environmental constraints of this ratio and model assumption.

4.4. Impact of El Niño–induced drought on forest productivity

The El Niño–induced drought has been found to cause substantial variation in Amazonian forest primary production (Asner et al. 2000) and net carbon budget (Tian et al. 1998). The 3-PG $NPP_{elniño}$ of 0.4 Pg C is comparable to Asner et al. (Asner et al. 2000) calculations of 0.3 Pg C yr^{-1} from El Niño events of 1982/83 and 1986/87 and 0.4 Pg C yr^{-1} 1990 through the 2-yr El Niño of 1991/92. These estimates are lower than the Tian et al. (Tian et al. 1998) results that showed the El Niño impact on NPP to be closer to 0.6–0.7 Pg C yr^{-1}, except for the 1982/83 (0.1 Pg C yr^{-1} impact on NPP). Recently, Potter et al. (Potter et al. 2001) also estimated a 0.4 PgC drop in NPP associated with historical El Niño events as well.

NPP is unchanged in the northwest (NW) portion of the basin because of drought, in agreement with the observations of Asner et al. (Asner et al. 2000), while throughout the central and southeastern regions NPP is severely reduced, often in excess of 70%. This is similar to the recent modeling of El Niño impact by Potter et al. (Potter et al. 2001), which conclude that NPP is reduced in some areas by 10% to 20%. In contrast, NPP is enhanced in some areas along the southwestern edge of the basin as a result of higher precipitation pattern to the south during El Niño years. In the context of deforestation, the results show that the southern boundary has higher growth rates during El Niño events; thus the potential regeneration is due to favorable El Niño phase climate.

Deforestation patterns are clustered across the region; therefore, climatic impacts and soil properties may have definite affects on reforestation rates as these different spatial patterns overlap with one another. Central forested regions are negatively impacted although differences in soil depth do not tend to exaggerate the El Niño drought effect other than decreasing NPP variability in northern mesic zones (Figure 10b), confirming other modeling work by Potter et al. (Potter et al. 2001). Changes in NPP in the central forested areas during El Niño years can have positive feedbacks in terms of increasing mortality, fuel loading, and wildfire occurrence due to litter and duff drying (Hirsch et al. 2004; Baker et al. 2004). This

hypothesis is consistent with the observation that 90% of accidental forest burning occurs during El Niño events (Cochrane et al. 1999).

4.5. Future directions

Models provide the opportunity to identify knowledge gaps. In this study, we found that soil water availability has a profound influence on long-term biomass accumulation likely to be related to periodic mortality. As 3-PG also estimates other stand characteristics such as stem density and mortality (due to self-thinning), the current calibrated model calibration could also be utilized to estimate natural tree attrition and downed woody debris buildup. Research indicates that El Niño climate in the central Amazon increases fire potential as a function of decreased fuel moisture. Spatial estimates of coarse woody debris could be derived from 3-PG to provide data for fuel loadings for subsequent simulations on fire behavior, frequency, and severity.

In addition to depletion of soil nutrients, deforestation changes site micrometeorology including increased surface temperature, decreased humidity, and increased soil irradiance (Giambelluca et al. 2003). These factors reduce site water balance and decrease likelihood of woody plant establishment and reforestation. Regional models rarely incorporate microscale factors such as deforestation because the spatial scale of the disturbance may be much less than the simulation unit. In this study, deforested areas were identified from the TRFIC data originally mapped at an 8-km spatial resolution. Selective logging techniques produce gaps in tropical forest canopies of approximately 220 m^2 per tree fall, which, although may not be detectable by moderate-resolution satellite observations, cumulatively affect forests through changes in canopy continuity and energy exchange (Asner et al. 2004). The 3-PG model was utilized to assess climate impacts on potential regeneration in deforested areas. However, spatial resolution differences between ground disturbance events and observation from satellites make the assessment of true damaged area difficult. This could partially explain the variable significant effects of climate and soil shown in Table 3. Future research will focus on assumptions about homogeneity in forest condition, soils, and climate for regional tropical forest production modeling.

5. Conclusions

Predicted NPP and ABA aboveground biomass accumulation after 20 and 100 yr is comparable to observed values derived from literature and MODIS sources. Using spatial inputs into the 3-PG model, we have shown the degree to which simulated forest productivity is controlled by soil moisture. The impact of the severe 1997/98 El Niño on simulated Amazon basin NPP is significant, equivalent to a reduction of almost 10% of total basin NPP relative to an "average" year. The impact of soil depth on simulated productivity indicated differential response between current deforested and forested sites under assumed soil depths of 2 and 5 m. This indicates a background pattern of water limits in which soil characteristics such as soil hydraulics may have a limited role. The results also suggest that secondary forests in the "arc of deforestation" are likely to be the most sensitive

in the Amazon basin to moisture stress, although affected positively during El Niño droughts.

References

Amthor, J. S., 2000: The McCree–de Wit–Penning de Vrie–Thornley respiration paradigms: 30 years later. *Ann. Bot.,* **86,** 1–20.

Asner, G. P., A. R. Townsend, and B. H. Braswell, 2000: Satellite observation of El Niño effects on Amazon forest phenology and productivity. *Geophys. Res. Lett.,* **27,** 981–984.

——, M. Keller, R. Pereira, J. C. Zweede, and J. N. M. Silva, 2004: Canopy damage and recovery after selective logging in Amazonia: Field and satellite studies. *Ecol. Appl.,* **14,** S280–S298.

Atlas, R. M., and R. Lucchesi, 2000: File specification for GEOS-DAS celled output. Goddard Space Flight Center, Greenbelt, MD, 41 pp. [Available online at http://www.ofps.ucar.edu/ghp/ceopdm/model/nasa_dao/filespec4.3.pdf).]

Baker, T., and Coauthors, 2004: Increasing biomass in Amazonian forest plots. *Philos. Trans. Roy. Soc. London,* **B359,** 353–365.

Brown, S., and A. E. Lugo, 1990: Tropical secondary forests. *J. Trop. Ecol.,* **6,** 1–32.

Carswell, E. E., and Coauthors, 2000: Photosynthetic capacity in a central Amazonian rain forest. *Tree Phys.,* **20,** 179–186.

Chambers, J. Q., J. dos Santos, R. J. Ribeiro, and N. Higuchi, 2000: Tree damage, allometric relationships, and above-ground net primary production in central Amazon forest. *For. Ecol. Manage.,* **152,** 1–12.

——, and Coauthors, 2004: Respiration from a tropical forest ecosystem: Partitioning sources and low carbon use efficiency. *Ecol. Appl.,* **14,** S72–S88.

Churkina, G., and S. W. Running, 1998: Contrasting climatic controls on the estimated productivity of different biomes. *Ecosystems,* **1,** 206–215.

Cochrane, M. A., A. Alencar, M. D. Schulze, C. M. Souza, D. C. Nepstad, P. Lefebvre, and E. A. Davidson, 1999: Positive feedbacks in the fire dynamic of closed canopy tropical forests. *Science,* **284,** 1832–1835.

Coops, N. C., R. H. Waring, and J. J. Landsberg, 1998: Assessing forest productivity in Australia and New Zealand using a physiologically-based model driven with averaged monthly weather data and satellite derived estimates of canopy photosynthetic capacity. *For. Ecol. Manage.,* **104,** 113–127.

Eamus, D., 1999: Ecophysiological traits of deciduous and evergreen woody species in the seasonally dry tropics. *Tree,* **14,** 11–16.

Emmons, L. H., and M. A. DuBois, 2003: Leaf-area index change across river-beach successional transects in south-eastern Peru. *J. Trop. Ecol.,* **19,** 473–477.

FAO/UNESCO, 1971: Soil map of the world. 1:5 000 000. United Nations Educational, Scientific, and Cultural Organization, Paris, France.

Fearnside, P. M., 1995: Potential impacts of climatic change on natural forests and forestry in Brazilian Amazonia. *For. Ecol. Manage.,* **78,** 51–70.

——, and W. M. Guimarães, 1996: Carbon uptake by secondary forests in Brazilian Amazonia. *For. Ecol. Manage.,* **80,** 35–46.

Feldpausch, T. R., M. A. Rondon, E. C. M. Fernandes, S. J. Riha, and E. Wandelli, 2004: Carbon and nutrient accumulation in secondary forests regenerating on pastures in Central Amazonia. *Ecol. Appl.,* **14,** S164–S176.

Gash, J. H. C., and C. A. Nobre, 1997: Climate effects of Amazonian deforestation: Some results from ABRACOS. *Bull. Amer. Meteor. Soc.,* **78,** 823–830.

Giambelluca, T. W., A. D. Ziegler, M. A. Nullet, D. M. Truong, and L. T. Tran, 2003: Transpiration in a small tropical forest patch. *Agric. For. Meteor.,* **117,** 1–22.

Goulden, M. L., S. D. Miller, H. R. da Rhocha, M. C. Menton, H. C. de Freitas, A. M. S. Figueira,

and C. A. D. de Sousa, 2004: Diel and seasonal patterns of tropical forest CO_2 exchange. *Ecol. Appl.,* **14,** S42–S54.

Granier, A., R. Huc, and S. T. Barigah, 1996: Transpiration of natural rain forest and its dependence on climatic factors. *Agric. For. Meteor.,* **78,** 19–29.

Guariguata, M. R., and R. Ostertag, 2001: Neotropical secondary forest succession: Changes in structural and functional characteristics. *For. Ecol. Manage.,* **148,** 185–206.

Hirsch, A. I., W. S. Little, R. A. Houghton, N. A. Scott, and J. D. White, 2004: The net carbon flux due to deforestation and forest re-growth in the Brazilian Amazon: Analysis using a process-based model. *Global Change Biol.,* **10,** 908–924.

Hodnett, M. G., M. D. Oyama, J. Tomasella, and A. de O. Marques Filho, 1996: Comparisons of long-term soil water storage behaviour under pasture and forest in three areas of Amazonia. *Amazonian Deforestation and Climate*, G. H. C. Gash et al., Eds., John Wiley, 287–306.

Honzak, M., R. M. Lucas, I. Do Amaral, P. J. Curran, G. M. Goody, and S. Amaral, 1996: Estimation of the leaf area index and total biomass of tropical regenerating forests: Comparison of methodologies. *Amazonian Deforestation and Climate*, G. H. C. Gash et al., Eds., John Wiley, 287–306.

Houghton, R. A., D. L. Skole, C. A. Nobre, J. L. Hackler, K. T. Lawrence, and W. H. Chomentowski, 2000: Annual fluxes of carbon from deforestation and regrowth in the Brazilian Amazon. *Nature,* **403,** 301–304.

IBGE, 1991: *Anuario Estatístico do Brasil*. Vol. 54, Fundãcao Instituto Brasileiro de Geografia e Estatística, 1024 pp.

Jipp, P. H., D. C. Nepstad, D. K. Cassel, and C. Reis de Carvalho, 1998: Forests and pastures of seasonally-dry Amazonia. *Climate Change,* **39,** 395–412.

Landsberg, J. J., 1986: *Physiological Ecology of Forest Production*. Academic Press, 198 pp.

——, and R. H. Waring, 1997: A generalized model of forest productivity using simplified concepts of radiation-use efficiency, carbon balance and partitioning. *For. Ecol. Manage.,* **95,** 209–228.

Laurence, W. F., P. M. Fearnside, S. G. Laurance, P. Delamonica, T. E. Lovejoy, J. M. Rankin-de Merona, J. Q. Chambers, and C. Gascon, 1999: Relationship between soils and Amazon forest biomass: A landscape-scale study. *For. Ecol. Manage.,* **118,** 127–138.

Malhi, Y., and Coauthors, 2002: An international network to monitor the structure, composition and dynamics of Amazonian forests (RAINFOR). *J. Veg. Sci.,* **13,** 439–450.

McCree, K. J., 1972: Test of current definitions of photosynthetically active radiation against leaf photosynthesis data. *Agric. Meteor.,* **10,** 443–453.

McMurtrie, R. E., H. L. Gholz, S. Linder, and S. T. Gower, 1994: Climate factors controlling the productivity of pine stands: A model-based analysis. *Ecol. Bull.,* **43,** 173–188.

McPhaden, M. J., 1999: The child prodigy of 1997–1998. *Nature,* **398,** 559–562.

Müller, M. M. L., W. M. Guimarães, T. Desjardins, and D. Mitja, 2004: The relationship between pasture degradation and soil properties in the Brazilian Amazon: A case study. *Agric. Ecosyst. Environ.,* **103,** 279–288.

Murray, F. W., 1967: On the computation of saturation vapor pressure. *J. Appl. Meteor.,* **6,** 203–204.

Nepstad, D. C., and Coauthors, 1994: The role of deep roots in the hydrological and carbon cycles of Amazonian forests and pastures. *Nature,* **372,** 666–669.

——, and Coauthors, 2002: The effects of rainfall exclusion on canopy processes and biogeochemistry of an Amazon forest. *J. Geophys. Res.,* **107,** 8085, doi:10.1029/2001JD000360.

New, M., M. Hulme, and P. Jones, 1999: Representing twentieth-century space–time climate variability. Part I: Development of a 1961–90 mean monthly terrestrial climatology. *J. Climate,* **12,** 829–856.

Pinker, R. T., and I. Laszlo, 1992: Modeling surface solar irradiance for satellite applications on a global scale. *J. Appl. Meteor.,* **31,** 194–211.

Potter, C., and V. Brooks-Genovese, 2003: LBA regional boundary for the legal Amazon of Brazil,

8-km: Data set. ORNL, xxx pp. [Available online at http://www.daac.ornl.gov and from Oak Ridge National Laboratory Distributed Active Archive Center, P.O. Box 2008Oak, Oak Ridge, TN 37831.]

——, E. A. Davidson, S. A. Klooster, D. C. Nepstad, G. H. de Negreiros, and V. Brooks, 1998: Regional application of an ecosystem production model for studies of biogeochemistry in Brazilian Amazonia. *Global Change Biol.,* **4,** 315–333.

——, S. Klooster, C. R. de Carvalho, V. B. Genovese, A. Torregrosa, J. D. Ungan, M. Bobo, and J. Coughlan, 2001: Modeling seasonal and interannual variability in ecosystem carbon cycling for the Brazilian Amazon region. *J. Geophys. Res.,* **106,** 10 423–10 446.

Raich, J. W., and Coauthors, 1991: Potential net primary productivity in South America. *Ecol. Appl.,* **4,** 399–429.

Roberts, J. M., O. M. R. Cabral, J. P. da Costa, A.-L. C. McWilliam, and T. D. de A. Sa, 1996: An overview of the leaf area index and physiological measurements during ABRACOS. *Amazonian Deforestation and Climate*, G. H. C. Gash et al., Eds., John Wiley, 287–306.

Running, S. W., R. R. Nemani, F. A. Heinsch, M. Zhao, M. Reeves, and H. Hashimotoa, 2004: Continuous satellite-derived measure of global terrestrial primary production. *Bioscience,* **54,** 547–560.

Runyon, J., R. H. Waring, S. N. Goward, and J. M. Welles, 1994: Environmental limits on net primary production and light-use efficiency across the Oregon transect. *Ecol. Appl.,* **4,** 226–237.

Saldarriaga, J. G., and R. J. Luxmoore, 1991: Solar energy conversion efficiencies during succession of a tropical rain forest in Amazonia. *J. Trop. Ecol.,* **7,** 233–242.

Salimon, C. I., and I. F. Brown, 2000: Secondary forests in western Amazonia: Significant sinks for carbon released from deforestation. *Interciencia,* **25,** 198–202.

Skole, D. L., and C. J. Tucker, 1993: Tropical deforestation and habitat fragmentation in the Amazon: Satellite data from 1978–1988. *Science,* **260,** 1905–1910.

Tian, H., J. M. Melillo, D. W. Kicklighter, A. D. McGuire, J. Helfrich, B. Moore III, and C. J. Vörösmarty, 1998: Effect of interannual climate variability on carbon storage in Amazonian ecosystems. *Nature,* **396,** 664–667.

Uhl, C., R. Buschbacher, and E. A. S. Serrao, 1988: Abandoned pastures in eastern Amazonia. I. Patterns of plant succession. *J. Ecol.,* **76,** 633–681.

Waring, R. H., J. J. Landsberg, and M. Williams, 1998: Net primary production of forests: A constant fraction of gross primary production? *Tree Phys.,* **18,** 129–134.

White, J. D., N. C. Coops, and N. A. Scott, 2000: Predicting broad-scale forest biomass in New Zealand: Estimate of indigenous New Zealand forest and scrub biomass from the 3-PG model. *Ecol. Modell.,* **131,** 175–190.

Williamson, G. B., W. F. Laurance, A. A. Oliveira, P. Delamônica, C. Gascon, T. E. Lovejoy, and L. Pohl, 2000: Amazonian tree mortality during the 1997 El Niño drought. *Conserv. Biol.,* **14,** 1538–1542.

Zeng, N., 1999: Seasonal cycle and interannual variability in the Amazon hydrologic cycle. *J. Geophys. Res.,* **104,** 9097–9106.

Zhao, M., F. A. Heinscha, R. R. Nemani, and S. W. Running, 2005: Improvements of the MODIS terrestrial gross and net primary production global data set. *Remote Sens. Environ.,* **95,** 164–176.